Colloids and Surfaces, 65 (1992) 257–272
Elsevier Science Publishers B.V., Amsterdam

Surfactant enhanced electro-osmotic separation of iron oxide ultrafines

Christine S. Grant, Eric J. Clayfield and Michael J. Matteson
Department of Chemical Engineering, Georgia Institute of Technology, Atlanta, GA 30332, USA

(Received 15 July 1991; accepted 25 November 1991)

Abstract

Electro-osmotic and vacuum separation techniques were applied to the study of naturally occurring iron oxide ($Fe_2O_3 \cdot H_2O$) ultrafine (≈ 2 μm) slurries. The absence of a significant particle zeta potential for electro-osmosis was overcome by increasing the concentration of potential-determining ions, through the addition of sodium hydroxide. The resulting electrostatic dispersion of the particles significantly reduced the rate and extent of hydraulic separation. Subsequent addition of small amounts of cetyl trimethylammonium bromide (CTAB; $5 \cdot 10^{-4}$–$5 \cdot 10^{-3}$ *M*) reflocculates the particles through electrostatic adsorption of CTAB ions, while maintaining sufficient zeta potential to utilize electro-osmotic separation techniques. In the case of NaOH and CTAB-treated samples, the final moisture content of an electro-osmotic filtered sample is over 40% lower than for an untreated vacuum separated sample. From electrophoretic measurements, the correlation between NaOH concentration and the extent of separation, the mechanism of adsorption, flocculation and subsequent dewatering is presented.

Keywords: Cetyl trimethylammonium bromide; electro-osmotic dewatering; flocculation; hydraulic dewatering; iron oxide; ultrafines; zeta potential.

Introduction

The effective separation of ultrafine particle dispersions is a critical problem area in mineral processing. In the final steps of mineral processing, fine particle dispersions, in the form of a tailing waste product, are generated, requiring adequate dewatering and disposal. The presence of ultrafines results in a significant reduction in the hydraulic permeability of the solid–liquid dispersion. In the case of ultrafines dewatering at the point where hydraulic separation becomes ineffective, thermal drying appears to be a viable alternative. However, thermal drying requires uneconomically large amounts of energy and may be unsuitable for heat-sensitive particles.

Correspondence to: C.S. Grant, Dept. of Chemical Engineering, Box 7905, North Carolina State University, Raleigh, NC 27695-7905, USA.

Sunderland [1] conducted a recent examination of industrial electrokinetic dewatering and thickening applications. Previous work by Lockhart [2] and others indicated that electrokinetic dewatering techniques can be effectively applied to fine-particle systems. Research on the use of electrokinetic dewatering has been conducted on densification of large lagoons of metal mine tailings [3], coal ultrafines separation [4], and dewatering sludge from sewage treatment plants [5–7]. The majority of electrokinetic separations research focuses on the continuous separation of fine particles from high-value product streams for more efficient transport and subsequent processing. Attempts to establish a relationship between fundamental parameters controlling electrokinetic separations (e.g. particle electric potential, state of aggregation and relative magnitude of surface charge) have been limited.

0166-6622/92/$05.00

Hydraulic dewatering is a term used to describe the removal of water under the influence of a pressure gradient; two major divisions are gravity drainage and applied pressure differential. Electro-osmotic dewatering describes the movement of a liquid relative to a stationary solid phase as a result of an externally applied electric field. The object of this paper is to present a study of the effect of two chemical additives (cetyl trimethylammonium bromide (CTAB) and sodium hydroxide) on the hydraulic and electro-osmotic dewatering behavior of iron oxide.

The base sodium hydroxide (NaOH) was utilized in this research to develop the required charge on the particle surface; the addition of a small amount of the base imparts a negative charge to the ochre. Supporting evidence for hydroxide ion adsorption was found from the large difference in the calculated slurry molarity and the actual measured slurry molarity based on pH measurements.

When CTAB is added to an iron oxide slurry containing NaOH, it performs the role of a flocculant; the electrostatic adsorption of the CTA^+ ions to the OH^- causes the hydrophobic tail of the surfactant to become oriented towards the aqueous phase. The hydrocarbon tails, in an effort to become removed from the aqueous phase, will become attracted to each other, thereby reducing the overall energy in the system. This hydrophobic attraction results in the flocculation of the iron oxide particles.

In an attempt to investigate variations in the specific resistance of the slurry following chemical treatment, a capillary suction time apparatus was used. Particular attention was paid to the surface characteristics of the ochre; zeta potentials of the ochre were measured in a series of experiments utilizing a microelectrophoretic apparatus. The driving force for the electro-osmotic separation is varied by altering the concentration of potential-determining ions of the iron oxide through the addition of CTAB and NaOH. A general model for adsorption and flocculation is presented to explain the experimental observations.

Investigations into the application of electro-osmotic dewatering to systems in the absence of a significant natural particle surface charge are limited. In contrast to earlier electro-osmotic separation studies, this paper investigates the difference in the magnitude of the change in both electro-osmotic and hydraulic dewatering. In this work we present a series of experiments performed at various NaOH and CTAB concentrations.

Combined field filtration

The parameters that govern ultrafines hydraulic dewatering include the pressure drop across both the filter medium and the material to be dewatered, the extent of particle flocculation, and associated packing properties of the solid. In electro-osmotic dewatering of ultrafines, the effectiveness of liquid removal is primarily a function of the zeta potential of the particles. The experiments in this study are designed to provide information that adequately describes how the aforementioned parameters interact during combined hydraulic and electro-osmotic dewatering.

In the present study, separation is achieved using vacuum and electro-osmotic dewatering. The total or overall flow rate in the system may be represented as

$$Q_{tot} = Q_{eo} + Q_{vac} \tag{1}$$

where Q_{tot} is the total volumetric flow rate, Q_{eo} the volumetric flow rate due to electro-osmosis, and Q_{vac} the hydraulic or vacuum contribution to the overall volumetric flow rate. Individual flow rates can be predicted theoretically as a function of experimentally measurable parameters. A quantitative relationship may be established between the electro-osmotic velocity of flow, the zeta potential, and the externally applied electric field [8,9].

Materials and methods

Minerals

Ochre is a naturally occurring inorganic iron oxide which is represented by the general chemical

formula, $Fe_2O_3 \cdot H_2O$ with associated water. It is a complex iron oxide mixture of the following primary minerals: goethite, $HFeO_3$; limonite, $HFeO_3 \cdot nH_2O$: and hematite, Fe_2O_3. Ochre is used primarily as a pigment in paints, construction materials, industrial chemicals, plastics and glass. The ochre pigments are lightfast, unreactive with solvents, resistant to bases and acids, and insoluble in water.

Aqueous ochre slurries with a fractional moisture content of 0.61 were obtained from the New Riverside Ochre Company in Cartersville, GA. New Riverside is a full-scale mining facility producing crude naturally occurring iron oxide pigments. The iron oxide slurries for this research were collected just prior to the rotary vacuum filtration process, a critical step in the mineral processing operation. These slurries did not contain any dispersants or flocculants which are used in subsequent processing steps. Previous analytical measurements on the ochre particles indicated an approximate mean particle size of 2.4 μm.

Chemicals

The cetyl trimethylammonium bromide (CTAB) from the Aldrich Chemical Company had a purity of 95% with the remaining 5% consisting of a stearyl compound. Aqueous solutions of CTAB at various concentrations were prepared by diluting the CTAB in distilled water from a Corning Mega-Pure System (MP-6A) distillation column. Sodium hydroxide stock solutions were prepared by dissolving Fisher Scientific NaOH pellets in distilled water.

Apparatus

The vacuum and electro-osmotic dewatering tests were performed in a batch dewatering cell consisting of a polyurethane Buchner funnel with the following dimensions: outer diameter, 10.69 cm; inner diameter, 10.26 cm; depth, 5.0 cm (see Fig. 1). The filter medium, Whatman no. 1 filter paper (9 cm in diameter), was placed over the perforations

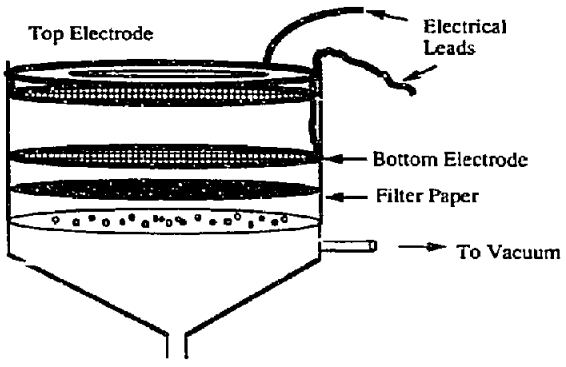

Fig. 1. Vacuum and electro-osmotic dewatering cell.

in the cell and secured by a polyurethane ring. The electrodes for the electro-osmotic studies were fabricated from bronze mesh screening. The bottom electrode was 9 cm in diameter with a continuous cord of solder on the outer edges to prevent screen fraying. The upper electrode had similar dimensions, with an additional piece of plexiglass (outer diameter, 8.75 cm; inner diameter, 6.87 cm; thickness, 1.25 cm) attached to it with epoxy to maintain electrode contact with the filter cake. During the initial stages of filter cake formation, the upper electrode was positioned on the partially consolidated filter cake to ensure sufficient electrical contact for the passage of current. The filter cake was not compressed by the weight of the upper electrode. Constant resistance to liquid flow was maintained during hydraulic and electro-osmotic dewatering experiments by positioning both electrodes in the cell. The filtrate was collected in a modified 100 ml Pyrex glass graduated cylinder.

The power source used in all electro-osmotic experiments was a VIZ Model WP-705 d.c. power supply, with a voltage range of 0–50 V. Most previous electro-osmotic dewatering research has been performed in a voltage range of 5–55 V [2,3,6] in order to maintain a low power requirement. The VIZ power supply also functioned as a dual digital display voltmeter/ammeter with a current range of 0.0–2.0 A. A Spectrum Vacu-trol Lab Regulator vacuum pump with a range of 0–760 mmHg provided the required hydraulic pressure for the vacuum dewatering phase.

Methods

Separation experiments

The ochre slurry was continuously mixed with a Stedfast Model SL 600 Stirrer using a pitched blade impeller. Initial measurements were made of the slurry pH and the weight of the slurry. Following the addition of a prepared liquid solution of either NaOH and/or CTAB, the pH measurements were repeated. The slurry was transferred to the dewatering cell and partially consolidated under constant vacuum with the volume of filtrate collected continuously recorded over a period of 30–50 min. In all tests, the measured vacuum range was 220–240 mmHg, with an average value of 230 mmHg. When 50 ml of liquid had been collected, the upper electrode was positioned on the filter cake.

After 20 min of hydraulic dewatering, when a firm filter cake had been formed, a constant potential of 35–45 V was applied to the system electrodes. The voltage and current across the filter cake were continually recorded during the dewatering test. The vacuum and potential were turned off when the flow of effluent stopped. The vacuum dewatering portion of the experiment ranged from 15 to 20 min. The electro-osmotic dewatering stage lasted approximately 20 min. The filter cake and the filtrate were retained for further physical and chemical property analysis.

All dewatering experiments were conducted at room temperature with the top of the cell at atmospheric pressure. The majority of the tests were carried out with the bottom electrode acting as the cathode to perform experiments under the influence of gravity. A few tests were undertaken with the anode as the bottom electrode to verify the polarity conditions for the best electro-osmotic effect.

Microelectrophoresis

Electrophoretic mobility measurements were performed with a Rank Particle Micro-Electrophoresis Apparatus Mark II using a thin-walled cylindrical cell with two platinum-blacked electrodes. Samples for the zeta potential studies were prepared from the effluent and the filter cake resulting from the electro-osmotic dewatering experiments. The dilute effluent–particle mixture was placed in a glass jar and dispersed for 5 min with a Fisher Model 300 Ultrasonic Dismembrator. The electrophoretic mobility values were taken as the average of 20 timings (10 in each direction) on different-sized particles. The electrophoretic mobility may be defined as the observed particle velocity divided by the potential gradient across the cell. The zeta potential was calculated using the rationalized form of the Smoluchowski equation:

$$\zeta = \frac{\mu_E \eta}{\epsilon} \tag{2}$$

where μ_E, ϵ and η are the electrophoretic mobility, permittivity and the viscosity of the fluid, respectively.

Specific resistance determination

A capillary suction time (CST) apparatus was used to analyze the specific resistance of the ochre slurry before and after chemical treatment. The capillary suction time apparatus has been developed to measure indirectly the specific resistance to filtration of a slurry [10,11]. The mechanism of the CST apparatus is a constant pressure filtration with the driving force provided by capillary suction. In CST operation, the slurry is poured into a circular metal collar reservoir resting on a piece of filter paper. Under the influence of capillary suction of a chromatography-grade filter paper, liquid is drawn out of the slurry, saturating a growing filter paper area. Capillary suction time is defined as the time required for the advancing liquid front to travel between the two metal probes in contact with the filter paper.

CST is directly proportional to the filtration characteristics of a slurry; a low CST corresponds to a low specific resistance to filtration and a relatively open-structured filter cake. Similarly, a high CST indicates a close-packed filter cake with a high specific resistance to filtration. The absolute

value of CST provides a good indication of the initial dewatering properties of the slurry. The change in CST values upon chemical addition provides insight into the changing nature of the slurry. In evaluating the changes in specific resistance to filtration, emphasis is placed on the changes in CST values relative to a starting value of an untreated sample. CST measurements were performed on the original ochre slurry and on the slurries treated with NaOH and CTAB.

Results and discussion

Data analysis

The data obtained from the dewatering test were in the form of volume of effluent as a function of time (in intervals ranging from 30 to 100 s). The dewatering time t was measured starting when the desired value of the vacuum was attained. During the initial stages of electro-osmotic dewatering, more frequent measurements of volume were taken in order to account for the sudden increase in the volume flow rate. The addition of aqueous sodium hydroxide and aqueous CTAB caused an increase in the initial moisture content of the slurry. In order to account for this variation, the volumetric data are presented as fractional moisture content data. The reported concentrations of NaOH and CTAB in the ochre slurry are based on the additivity of the original volume of liquid in the slurry and the volume of aqueous surfactant and base added.

The driving force for electrokinetic separations is usually defined in terms of the applied voltage per unit distance (e.g. V cm^{-1}). In this research the thickness of the final filter cake is approximately 1 cm. However, over the duration of the dewatering experiments, the distance between the electrodes is reduced slightly due to a reduction in the volume of the filter bed upon the removal of filtrate. Therefore, the driving force for electro-osmosis is presented as + or − the applied voltage; the sign on the potential corresponds to the polarity of the bottom electrode (e.g. +35 V).

Untreated iron oxide slurry

Preliminary characterization of the naturally occurring ochre slurry (i.e. as received from the processing facility) indicates to what extent the particles must be chemically modified to facilitate an electro-osmotic separation. In the current research the slurry samples were obtained from the processing facility over a period of 2 years. Although there was not a large variation in the hydrophobicity and the charge of the particles, there was a slight difference in the state of aggregation. Periodic checks of untreated slurry dewatering behavior were performed in between the chemical additive tests as a check with the initial experimental data.

Subsequent electro-osmotic dewatering experiments were performed to determine whether the zeta potential of the natural ochre particles was high enough to generate an electro-osmotic enhancement. A direct current of 35 V, with the lower electrode acting as the cathode, was applied to the filter cake; the results of this condition are indicated in Fig. 2. The absence of an abrupt change in the slope of the fractional moisture content vs. time curve, upon application of a

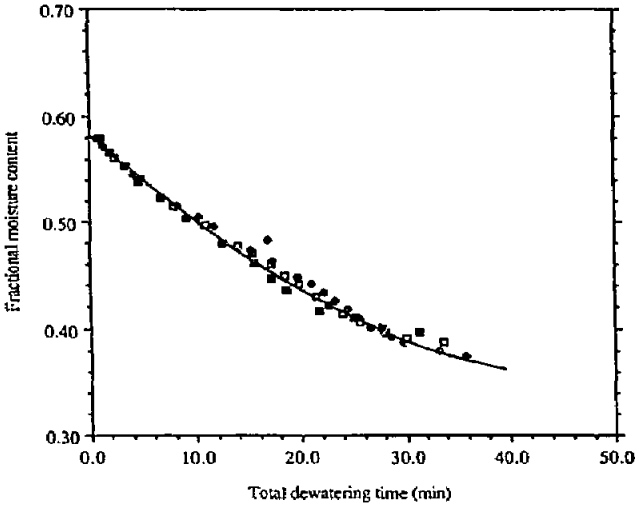

Fig. 2. Electro-osmotic separation of naturally occurring ochre slurry with applied potential of 35 V (bottom electrode as anode or cathode): □, untreated slurry, −35 V; ◆, untreated slurry, +35 V; ■, untreated slurry, 0 V.

potential, indicates there is not a significant electro-osmotic enhancement. A reversal of the electrode polarity (bottom electrode acting as the anode) produces a similar result, indicating the need for generation of charge at the surface.

The proposed absence of natural particle charge is verified by the zeta potential measurements. When the electrophoretic mobility of the untreated slurry was measured at varying applied potential and currents, no particle movement was observed, corresponding to an electrophoretic mobility of zero. These findings confirm that the particles are neutral in charge; they also establish that the natural slurry is in the vicinity of, or at the point of, zero charge. In this research, the measured pH of the untreated slurry in the absence of a significant surface charge is 6.3, which is in close proximity to the reported literature values [12] of the point of zero charge (PZC) for goethite (pH 6.7).

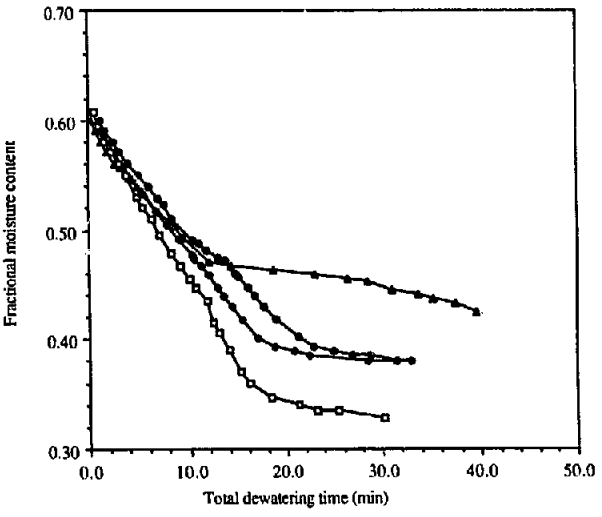

Fig. 3. Electro-osmotic separation experiments for Type 1 natural ochre slurries (concentration series with CTAB; applied potential, 35 V; bottom electrode as the cathode): △, $6.3 \cdot 10^{-3}$ *M* CTAB; ●, $5.9 \cdot 10^{-4}$ *M* CTAB; ◆, $4.3 \cdot 10^{-4}$ *M* CTAB; □, $3.4 \cdot 10^{-4}$ *M* CTAB.

Adsorption behavior of ochre samples

Earlier research on ochre slurries from New Riverside Ochre Company resulted in the classification of the dispersions [13] into two slurry types (Type 1 and Type 2) based on the varying degree of surface adsorption and natural surface charge. In this earlier work [13], addition of small amounts of CTAB ($3 \cdot 10^{-3}$ *M*) produced an increase in the rate of dewatering when a potential of 35 V was applied. The enhancement due to electro-osmosis occurred when the bottom electrode functioned as the anode. Supporting evidence that this was an electro-osmotic phenomenon and was not due to electrode heating or evaporation was found when electrode polarity reversal caused a decrease in the original dewatering rate. Figure 3 illustrates that when the bottom electrode functions as the cathode, an increase in the CTAB concentration from $3.4 \cdot 10^{-4}$ to $6.3 \cdot 10^{-3}$ *M* causes a significant increase in the final fractional moisture content.

The adsorption of CTAB in the preliminary dewatering study may be attributed to the dipole–dipole interactions between the particle and the cationic surfactant. The underlying assumption of this mechanism is that although the natural ochre has a zeta potential of zero, the highly electronegative oxygen atoms in the ochre surface attract the CTA^+ ions. Subsequent hydrophobic adsorption of CTA^+ ions results in a net positive charge on the ochre; this results in an electro-osmotic enhancement of the flow when the bottom electrode functions as the anode.

The second ochre slurry sample (Type 2) was similarly uncharged, as evidenced by the lack of an electro-osmotic effect regardless of the polarity of the bottom electrode. In contrast to the Type 1 slurry, Type 2 slurry samples did not demonstrate an electro-osmotic enhancement upon CTAB addition. This behavior could be caused by a change in the dipole–dipole interaction between the CTA^+ ions and the ochre surface ions. This sudden change in the effect of CTAB adsorption on electro-osmotic dewatering performance may be caused by differences in the geological formation and the subsequent mining of the ochre.

Initial dewatering experiments and electrophoretic mobility measurements on the untreated slurry in the current research characterized the ochre particles as uncharged. The ochre slurry in

the present study exhibited the surface characteristics of a Type 2 slurry and the addition of CTAB provided no electro-osmotic enhancement with application of +35 V. There is still the absence of an electro-osmotic effect when the polarity of the system is reversed and the bottom electrode acts as the cathode (−35 V). A measured zeta potential of zero indicates that the ochre system is still at the PZC with no adsorption of the surfactant to the ochre particles.

Effect of CTAB on dewatering

Experiments were conducted to investigate the effects of the CTAB concentration on both the hydraulic and electrical dewatering behavior of ochre slurries at constant pressure and temperature. Figure 4 illustrates that for vacuum filtration only when the concentration of CTAB is increased by a factor of 2, is there an enhancement in the rate and extent of hydraulic filtration. The increased dipole–dipole interactions in the Type 2 slurry may result in the development of a hydrophobic surface; this causes the particles to flocculate as the concentration of CTAB is increased.

Further assessment of the hydraulic dewatering behavior of the surfactant-treated slurry was carried out using the CST apparatus. The specific resistance to filtration is related, based on first principles, to the capillary pressure drop which can be qualitatively measured by capillary suction time:

$$\Delta P_c = \frac{2\gamma \cos\theta}{r_i} \tag{3}$$

where γ is the surface tension, θ is the contact angle, and r_i is the radius of the capillary. The difference in CST is, therefore, proportional to the change in the capillary pressure drop in the dewatering slurry. The addition of a small amount of CTAB ($5 \cdot 10^{-4}$–$2 \cdot 10^{-3}$ M) results in a decrease in CST values from the untreated slurry value of 86 s to a value of 62 s for the treated slurry (the CST of pure water is 6 s). The addition of CTAB causes a decrease in the surface tension, causing the value of ΔP_c in Eqn (3) to decrease; this facilitates hydraulic dewatering. A change in both CST and surface tension as a function of CTAB concentration is shown graphically in Fig. 5.

Effect of NaOH on electro-osmotic dewatering

For iron oxides, the selective adsorption of potential-determining OH^- and H^+ ions by the

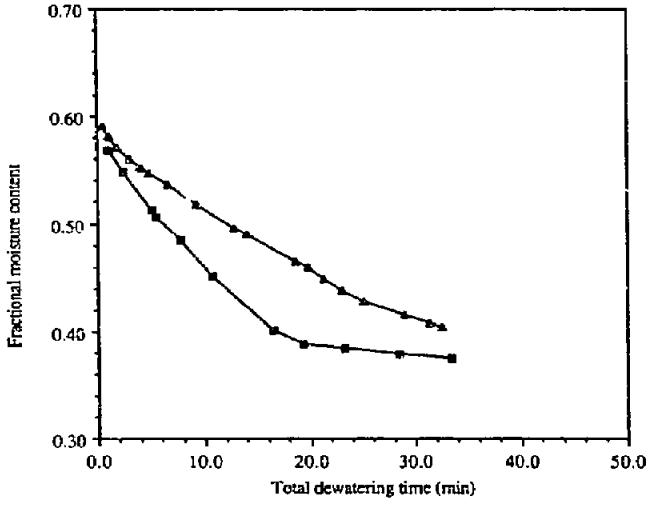

Fig. 4. The effect of varying CTAB concentration under conditions of vacuum dewatering: ■, $1.1 \cdot 10^{-3}$ M CTAB, 0 V; ▲, $5.2 \cdot 10^{-4}$ M CTAB, 0 V.

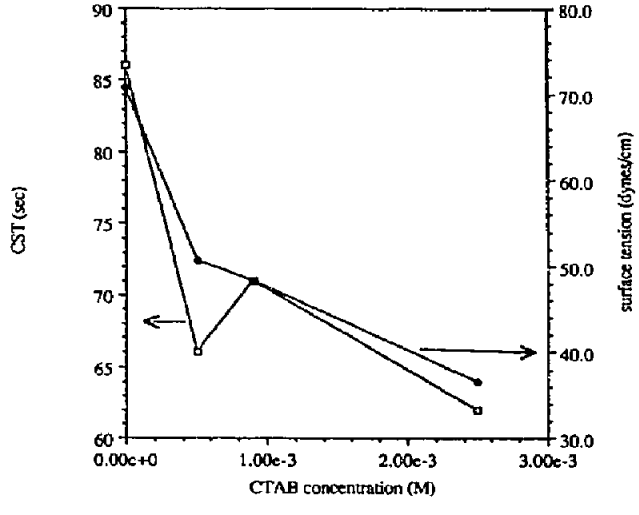

Fig. 5. Relationship between capillary suction time (CST) (□), surface tension (dyn cm^{-1}) (●), and CTAB concentration. CST data from prepared ochre slurries, surface tension measurements performed on filtrate samples.

particles can be controlled by the addition of acids or bases and measured by changes in the pH of the slurry [9]. The addition of sodium hydroxide has been determined, by earlier studies, to generate an electro-osmotic effect on iron oxide particles [13,14]. In the current study, the addition of NaOH increases the pH of the system, with the corresponding zeta potential becoming increasingly negative (see Fig. 6).

A series of tests with NaOH addition (i.e. in the absence of CTAB) was conducted with hydraulic dewatering as the sole driving force in order to observe the extent of dewatering at various concentrations of sodium hydroxide. Figure 7 illustrates that under the influence of vacuum alone, an increase in the NaOH concentration from $5.3 \cdot 10^{-3}$ to $7.3 \cdot 10^{-3}$ M results in a significant reduction in the final moisture content and a corresponding decrease in the slope of the fractional moisture content vs. time. In the experiments conducted with NaOH alone, the reduction in hydraulic dewaterability is attributed to the dispersal of the iron oxide particles owing to the surface adsorption of hydroxide ions. The cake formation with smaller particles results in a less permeable bed.

A demonstration of the performance of sodium-hydroxide-treated slurries under the conditions of electro-osmotic dewatering is also presented in

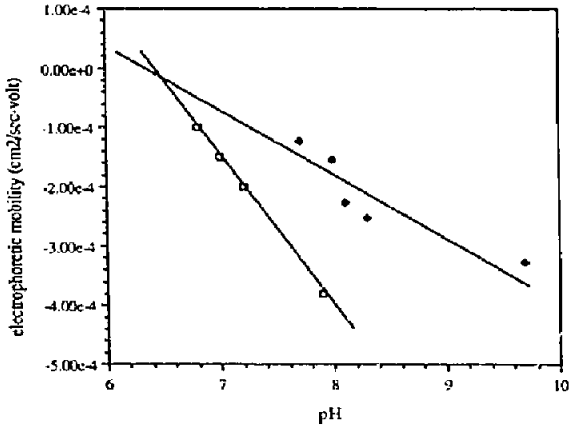

Fig. 6. Comparison of literature electrophoretic mobilities for hematite ((□), Iwasaki et al. [12]) and measured values (◆) for naturally occurring ochre in filtration effluent.

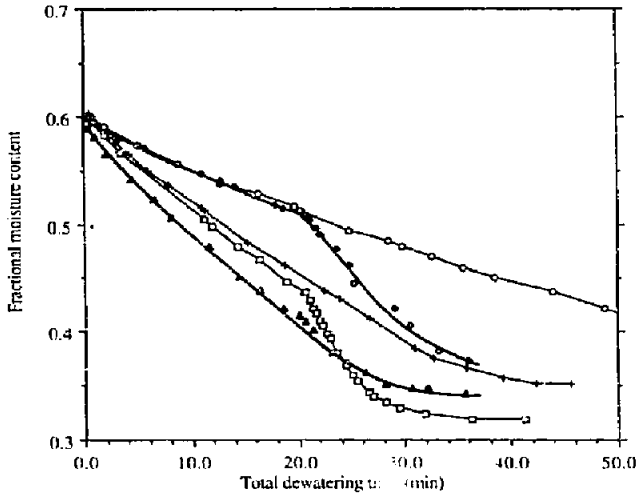

Fig. 7. Relationship of NaOH concentration (0 M–$7.3 \cdot 10^{-3}$ M) with vacuum-only and vacuum plus electro-osmotic dewatering (0 M CTAB): ▲, untreated, 0 V; □, $5.3 \cdot 10^{-3}$ M NaOH, −45 V; +, $5.3 \cdot 10^{-3}$ M NaOH, 0 V; ◇, $7.3 \cdot 10^{-3}$ M NaOH, −45 V; ○, $7.3 \cdot 10^{-3}$ M NaOH, 0 V.

Fig. 7. When compared to experiments conducted on the untreated ochre slurries, which lack a sufficient electrical charge to produce an electro-osmotic effect, NaOH-treated slurries show an improvement in the electro-osmotic portion. Closer analysis of Fig. 7 demonstrates that at concentrations of $5.3 \cdot 10^{-3}$ and $7.2 \cdot 10^{-3}$ M the reduction of the hydraulic flow with sodium hydroxide is overcome by the electro-osmotic contribution to the overall dewatering. The final moisture content of the NaOH-treated slurries (Fig. 7) after 16 min of combined vacuum and electro-osmotic dewatering is lower than the final moisture content of the untreated slurry. However, at higher NaOH concentration ($7.3 \cdot 10^{-3}$ M) the generation of an electro-osmotically enhanced rate of liquid removal does not overcome the hydraulic reduction caused by the electrostatic dispersal of particles.

In this research, a quantitative analysis of hydroxide ion adsorption and the resulting variations of zeta potential was conducted An estimate of the extent of hydroxide ion adsorption is made by comparing the theoretical molarity to the actual filtrate molarity. The theoretical filtrate hydroxide molarity (and theoretical pH) is calculated based upon the quantity of liquid present in the slurry

and the known amount of NaOH added. By measuring the pH of the filtrate, an estimate of the concentration of hydroxide ion in the liquid phase is determined. The difference between the theoretical hydroxide concentration and the actual concentration denotes the relative quantity of OH^- ion adsorption. Inspection of the table of theoretical NaOH concentrations and the moles of NaOH adsorbed (Table 1) clearly indicates that most of the hydroxide ions are adsorbed onto the particles. The remaining OH^- ions are present in the liquid phase and cause a change in the conductivity of the filtrate as measured during the microelectrophoresis.

A change in zeta potential also verifies the adsorption of hydroxide ions. A study of the electrophoretic mobility of the ochre particles correlates well with the observed enhanced flow rates during electro-osmotic dewatering. Rank microelectrophoretic studies of NaOH-treated iron oxide slurries, yield electrophoretic mobilities ranging from $1.2 \cdot 10^{-8}$ to $3.3 \cdot 10^{-8}$ $m^2 V^{-1} s^{-1}$, with corresponding zeta potentials of -15.4 to -42.3 mV. Figure 6 compares the electrophoretic mobilities of the ochre as a function of pH measured by the Rank microelectrophoresis apparatus with electrophoretic mobilities of hematite reported by Iwasaki et al. [12]. Although the electrophoretic mobility values in the current study are higher than hematite values reported in the literature [12,15], the pH in the vicinity of the PZC was 6.3 and is in good agreement with the literature PZC values (pH 6.7). An important difference in the aforementioned electrophoretic mobility results is that the ochre utilized in this research is a combination of a variety of iron oxides, not pure hematite.

Synergistic effect of base and surfactant

At a specific concentration of NaOH in the ochre slurry, increasing amounts of CTAB were added to the ochre slurry. The CTAB concentration series was then repeated at different starting concentrations of NaOH in the ochre slurry. The electrostatic adsorption of surfactant reduces the dispersing effect that base has on the slurry through reflocculation of the ochre particles. The adsorption of CTA^+ ions permits the particle surface to retain a sufficient zeta potential from the hydroxide ion adsorption to generate an electro-osmotic effect. However, the adsorption of an excess of CTA^+ ions can significantly reduce the rate and extent of electro-osmotic dewatering by increasing the zeta potential to zero and causing a zeta potential to become positive through multilayer adsorption.

Table 2 summarizes the range of additive concentrations and the resulting zeta potential used in the current study. The best condition for hydraulic and electro-osmotic separation necessitates a balance between the state of particle aggregation, which affects the hydraulic contribution, and the magnitude of the zeta potential, which determines the electro-osmotic enhancement.

At $9.8 \cdot 10^{-3}$ *M* NaOH concentration, the highest base concentration used in this series, the CTAB concentration is increased from $5.4 \cdot 10^{-4}$ *M* to a value of $3.0 \cdot 10^{-3}$ *M*. When compared to untreated

TABLE 1

Theoretical and actual pH values as an indication of hydroxide ion adsorption

Theoretical NaOH conc.	Theoretical pH	Actual pH	Measured NaOH conc.	Moles OH^- ions "adsorbed"
$9.3 \cdot 10^{-4}$	11.0	7.7	$5.0 \cdot 10^{-7}$	$9.3 \cdot 10^{-4}$
$2.3 \cdot 10^{-3}$	11.4	8.0	$1.0 \cdot 10^{-6}$	$2.3 \cdot 10^{-3}$
$5.3 \cdot 10^{-4}$	11.7	8.1	$1.3 \cdot 10^{-6}$	$5.3 \cdot 10^{-4}$
$8.1 \cdot 10^{-3}$	11.9	8.3	$2.0 \cdot 10^{-6}$	$8.1 \cdot 10^{-3}$
$9.9 \cdot 10^{-3}$	12	9.7	$5.0 \cdot 10^{-5}$	$9.9 \cdot 10^{-3}$

TABLE 2

Zeta potential (in mV) of ochre samples from filter cake as a function of NaOH and CTAB concentrations

NaOH conc. (M)	CTAB conc. (M)				
	0.0	$5.0 \cdot 10^{-4}$	$9.0 \cdot 10^{-4}$	$2.5 \cdot 10^{-3}$	$5.0 \cdot 10^{-3}$
$9.0 \cdot 10^{-4}$	−15.5	−15.7	−14.9	−15.0	+8.2
$2.5 \cdot 10^{-3}$	−19.9	−21.8	−33.7	−17.7	−20.3
$5.0 \cdot 10^{-3}$	−29.1	−36.1	−32.6	−18.2	−14.5
$7.0 \cdot 10^{-3}$	−32.4	−22.3	−35.7	−30.8	−21.6
$9.0 \cdot 10^{-3}$	−42.1	−35.4	−43.0	−40.7	−15.0

slurry under vacuum alone conditions (Fig. 8), in the hydraulic portion of the curves there is an increase in the rate and extent of dewatering as the concentration of CTAB is increased. Earlier tests indicate that NaOH concentrations of $9 \cdot 10^{-3}$ M cause a significant decrease in the dewaterability of the slurry in the absence of surfactant. A comparison of this test with base alone to one with a small amount of CTAB ($5.4 \cdot 10^{-4}$ M) supports the proposed adsorption mechanism which describes the reflocculation of base-dispersed particles through hydrophobic attraction of the adsorbed CTAB tails.

At a dewatering time of 20 min, an applied potential of −45 V (Fig. 9) causes an electro-osmotic enhancement over the entire CTAB concentration range at a constant NaOH concentration of $9.8 \cdot 10^{-3}$ M. However, the rate of electro-osmotic enhancement is not as pronounced at the lowest CTAB concentration ($5.4 \cdot 10^{-4}$ M). For the ochre slurry at $9.8 \cdot 10^{-3}$ M NaOH, the lowest final fractional moisture content of 0.351 is achieved at a CTAB concentration of $3.0 \cdot 10^{-3}$ M. In the range of concentrations studied in this system, the combined electro-osmotic improvement and high hydraulic permeability resulted in significant reductions in the extent of dewatering.

The relationship between measured zeta poten-

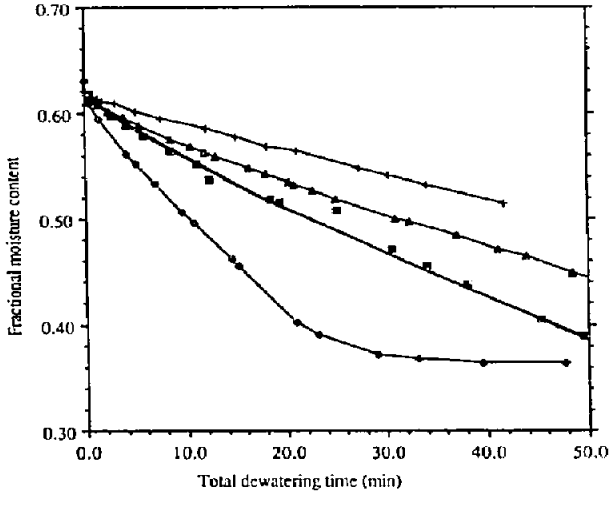

Fig. 8. Constant NaOH concentration of $9.8 \cdot 10^{-3}$ M under conditions of vacuum-only dewatering, varying CTAB concentration from $5.4 \cdot 10^{-4}$ to $3 \cdot 10^{-3}$ M: +, 0.0 M CTAB; ▲, $5.4 \cdot 10^{-4}$ M CTAB; ■, $8.5 \cdot 10^{-4}$ M CTAB; ◇, $3.0 \cdot 10^{-3}$ M CTAB.

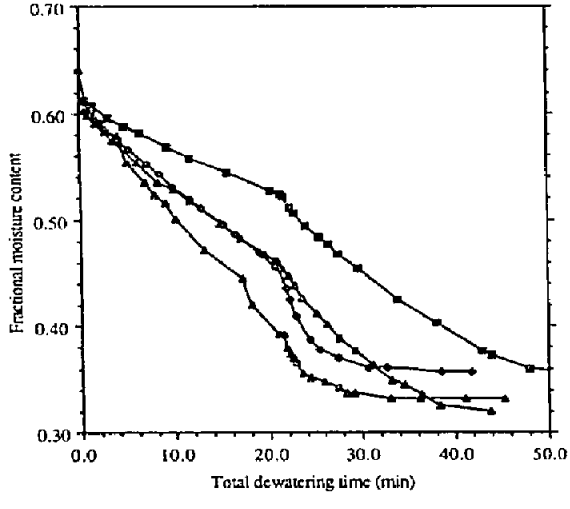

Fig. 9. Electro-osmotic dewatering at NaOH concentration of $9.8 \cdot 10^{-3}$ M with applied potential of −45 V: ■, $5.2 \cdot 10^{-4}$ M CTAB; ▲, $8.5 \cdot 10^{-4}$ M CTAB; ◇, $3.0 \cdot 10^{-3}$ M CTAB; △, $4.8 \cdot 10^{-3}$ M CTAB.

tial and CTAB molarity is shown in Fig. 10 for increasing concentrations of NaOH. There is no appreciable change in the zeta potential until the CTAB concentration is greater than $3 \cdot 10^{-3}$ *M*. The slope of the dewatering curve over the entire range of surfactant concentration supports the mechanism of hydroxide adsorption in all cases. Figure 10 reveals that the least negative value of zeta potential occurs at the highest CTAB concentration used in this study ($5 \cdot 10^{-3}$ *M*) at both concentrations of NaOH. The zeta potential becomes positive at the lowest NaOH concentration. This experimentally measured charge reversal suggests the mechanism of multilayer adsorption with excess CTAB.

The percentage increase in the extent of dewatering can be calculated from the difference in final moisture content of the untreated and chemically modified ochre slurries. The final moisture content was evaluated at a total dewatering time of 30 min. This corresponds to the time at which the majority of the dewatering experiments have reached a minimum in the liquid removal rate. Figure 11 indicates that as the concentration of NaOH is increased from $9 \cdot 10^{-4}$ to $9 \cdot 10^{-3}$ *M* the overall decrease in the final moisture content (without CTAB) varies from 4.5 to 34.5%. Although there

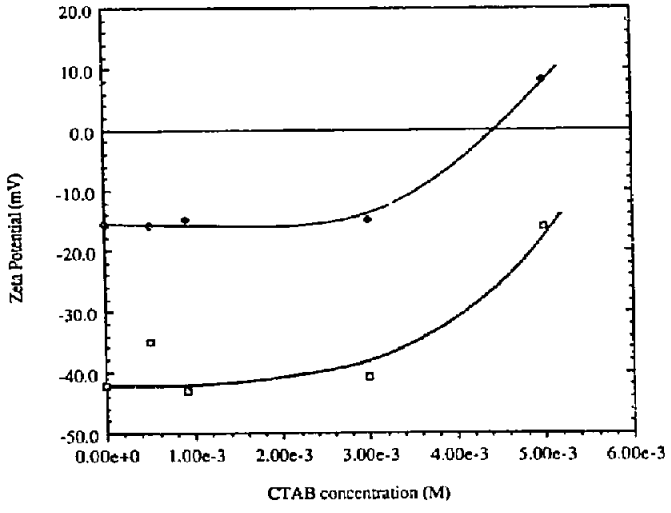

Fig. 10. Measured zeta potential as a function of CTAB concentration at NaOH concentrations of $9 \cdot 10^{-3}$ *M* (□) and $9 \cdot 10^{-4}$ *M* (◆).

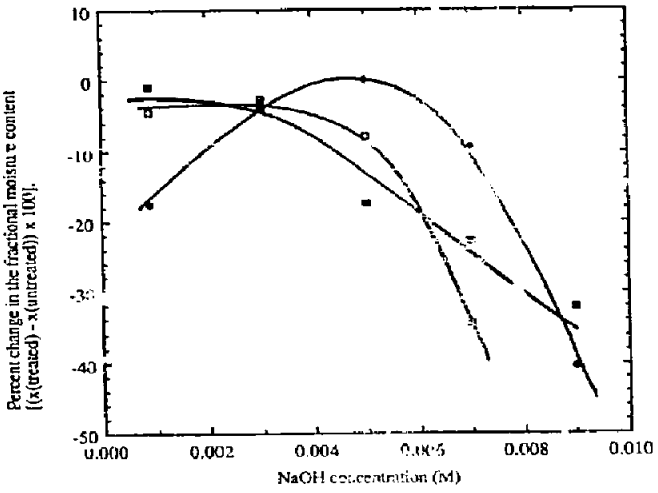

Fig. 11. Percentage change in fractional moisture content from untreated ochre slurry to NaOH/CTAB treated slurry at $t = 30$ min (untreated slurry, vacuum dewatered; treated slurry, vacuum and electro-osmotic dewatered): □, 0 *M* CTAB; ◆, $5 \cdot 10^{-4}$ *M* CTAB; ■, $9 \cdot 10^{-4}$ *M* CTAB.

is not a significant correlation between the CTAB concentration and the percentage increase in the extent of separation, similar behavior is exhibited at CTAB concentrations of $5 \cdot 10^{-4}$ and $9 \cdot 10^{-4}$ *M*.

The observed adsorption mechanism of the iron oxide in the presence of NaOH and CTAB is supported by flotation studies conducted on iron oxide particles. Iwasaki et al. [12] investigated the flotation behavior of hematite with 10^{-4} *M* octadecylammonium chloride and sodium octadecylsulfate over the entire range of pH values. Their research indicated an increase in the surface activity of the longer-chained collectors with increasing pH, suggesting two mechanisms of surfactant interactions with the iron oxide surface: (1) a lateral interaction of hydrocarbon chains of the adsorbed organic ions, and (2) the electrostatic attraction between the iron oxide surface and the collector ion [12].

Determination of electro-osmotic flow rates from experimental data

The combined vacuum and electro-osmotic flow rates have been measured at the point of application of a potential and for several minutes there-

after. The value of Q_{eo} (the electro-osmotic flow rate), is determined by selecting a time for which there are data from the vacuum portion to subtract from the combined flow rate value, Q_{tot}. A plot of the filtrate volume vs. time yields the slope of this curve when the potential is applied. The information obtained from vacuum dewatering experiments is used to determine what this flow rate would be at the point of application of a potential.

Generally, the addition of electro-osmotic flow more than doubles the flow solely under vacuum conditions. An increase in the zeta potential through the addition of potential-determining OH^- ions improves the overall flow rate by slightly over 50% in the concentration range $9 \cdot 10^{-4}$ to $9 \cdot 10^{-3}$ M NaOH through an increase in the zeta potential.

The electro-osmotic efficiency

The amount of electrical energy expended may mitigate the overall benefits of electro-osmotically enhanced flow. An electro-osmotic efficiency is defined based on the fraction of electrical energy which is actually used to drive the fluid out of the slurry relative to the total energy input for the separation. The electro-osmotic flow rate at the beginning of the electro-osmotic portion of the run Q_{eo} at the point of application of a potential may be determined from experimental results using Eqn (1). The experimental value is compared with the theoretical value of the electro-osmotic flow rate in a filter cake. The theoretical value of the electro-osmotic flow rate is based on the filter bed modeled as a bundle of capillaries:

$$Q_{eo} = \frac{\Phi \zeta \epsilon A_T}{L\mu} \tag{4}$$

where L is the length of the capillary, ϵ is the porosity, μ is the viscosity of the filtrate, Φ is the total potential drop, ζ is the zeta potential of the particles, and A_T the cross-sectional area of the cake available for flow. All of the parameters in Eqn (4) may be determined independently at $t = 0$.

Taking into account the effect of surface conductance, the apparent cake thickness $(L + L_R)$ will be experimentally larger than the actual measured value of the cake thickness L. Incorporation of the surface conduction effects in the actual conductivity term K yields

$$K + \frac{2K_s}{a} \tag{5}$$

where K is the liquid conductivity, K_s is the surface conductivity and a is the capillary radius. Incorporating the above correction for surface conductance into Eqn (4) yields:

$$Q_{eo,exp} = \frac{i\zeta}{[K + (2K_s/a)]\mu} = \frac{\Phi \zeta \epsilon A_T}{(L + L_R)\mu} \tag{6}$$

The electro-osmotic efficiency can be defined as

$$E_{eo} = \frac{(Q_{eo,exp})}{(Q_{eo,theor})} = \frac{L}{L + L_R} = \frac{K}{K + (2K_s/a)} \tag{7}$$

The value of L is known from the measured values of filtrate volume at the beginning and the end of application of an electric potential from the following relation:

$$V = V_f - V_i = L\epsilon_0 A_T \tag{8}$$

where V is the volume of the liquid removed, V_f is the volume of the liquid in the final filter cake, V_i is the initial volume of liquid in the slurry and ϵ_0 is the porosity of the cake. The value of $L + L_R$ is found from

$$L + L_R = \frac{\Phi \zeta \epsilon A_T}{\mu(Q_{eo,exp})} \tag{9}$$

Figure 12 indicates how average values of K_s and E_{eo} vary with CTAB concentration. An increase in the concentration of CTAB results in a reduction in the surface tension, allowing more water to be removed hydraulically. In contrast, an increase in the CTAB concentration has a detrimental effect on the electro-osmotic efficiency owing to an increase in the surface conductivity.

The experimentally calculated surface conductivity values are higher than the literature values for

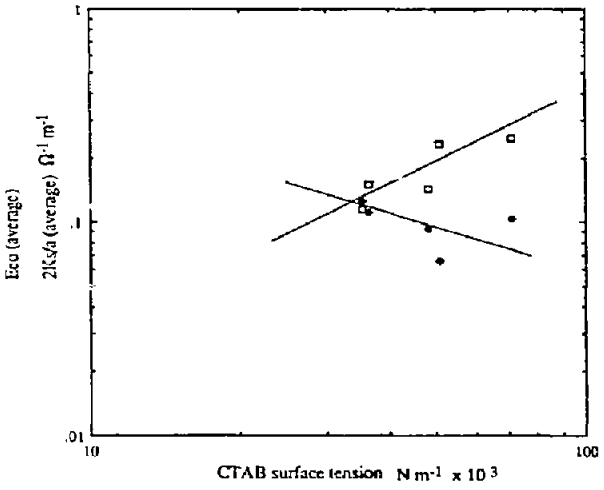

Fig. 12. Average electro-osmotic efficiency as a function of CTAB surface tension: □, E_{co} (average); ◆, $2K_s/a$ (average).

similar systems. For example, for monolayers of stearic acid in distilled water, K_s is $(3.5–3.8)\cdot 10^{-8}\,\Omega^{-1}$ [16]. The surface conductivity observed in this research may be caused by the concentrations of CTAB added to the ochre system. The ochre sample may already have a high conductivity with CTAB; this is evidenced by the calculated K_s value of $\approx 7\cdot 10^{-8}\,\Omega^{-1}$ at zero CTAB concentration.

Figure 13 shows how the average surface conductivity also increases with NaOH concentration

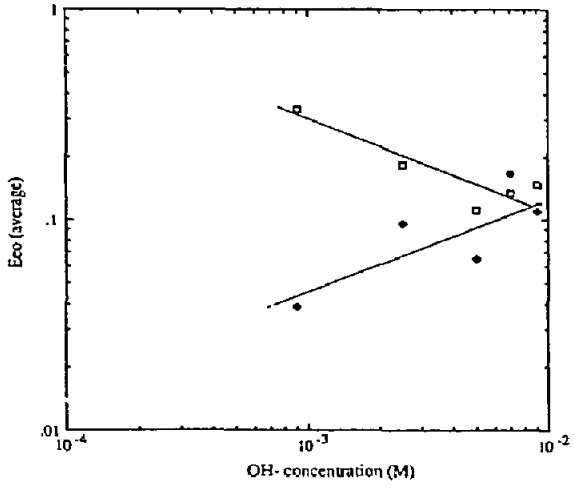

Fig. 13. Effect of increasing NaOH concentration on calculated electro-osmotic efficiency and surface conductance: □, E_{co} (average); ◆, $2K_s/a$ (average).

with an associated reduction in the electro-osmotic efficiency until the sodium hydroxide concentration is equal to $5\cdot 10^{-3}\,M$ after which there is a slight rise. This could be due to the increasingly negative zeta potential overcoming losses in conductivity from CTAB alone.

Electrokinetic effects

In electrical dewatering of aqueous slurries, the application of a d.c. electric field results in four phenomena: electrophoresis, electro-osmosis, electrolysis and coulombic heating. Based on the concentrated nature of the ochre slurries and the orientation of the experimental cell, electrophoretic dewatering is negligible in terms of the overall dewatering rate. The quantity of coulombic heat produced is proportional to the conductivity of the slurry and the square of the current [17]. The efficient use of energy for electro-osmotic separations also requires a low conductivity to minimize the consumption of electrical power [18]. The maximum conductivity for minimal coulombic heating is a function of the geometry of the dewatering device and the specifications of the process materials.

The application of a direct current causes electrolysis reactions to occur at the electrodes. At the anode the possible reactions are [19]

$$6H_2O \rightarrow O_2(g) + 4H_3O^+ + 4e^- \quad (10)$$

$$M \rightarrow M^{n+} + ne^- \quad (11)$$

where M is the metal of electrode construction. Equation (11) describes the corrosion of the anode. At the cathode the following reactions may occur:

$$2H_2O + 2e^- \rightarrow H_2 + 2OH^- \quad (12)$$

$$2H_3O^+ + 2e^- \rightarrow H_2O + 2H_2(g) \quad (13)$$

$$M^{n+} + ne^- \rightarrow M \quad (14)$$

The bronze electrodes used in this research were primariiy copper (over 80%). The dissolution of a copper anode would produce copper ions via the

following reaction:

$$Cu \rightarrow Cu^{2+} + 2e^- \quad (15)$$

Because this reaction has a lower potential than the H_2O reaction (Eqn (10)), the predominant anodic reaction is dissolution of copper. The copper ions may react in the filter bed to produce copper hydroxides, copper oxides or copper bromide in the presence of CTAB. The reduction of Cu^{2+} (Eqn (14)) at the cathode will occur only if the metal ions from the anodic reaction reach the cathode.

During several dewatering experiments, a brown filtrate was observed during the electro-osmotic portion of the process (see Table 3). In some instances the filtrate cleared up during the dewatering test (≈40 min), while in other cases the color remained days or weeks after the test was completed. The presence of a lingering brown filtrate suggests that an electrochemical reaction occurs during electro-osmosis. In all cases the observation of colored drops from the dewatering cell would occur only after the potential was applied to the system. In the range of occurrence of a colored filtrate the CST results are high, corresponding to maximum dispersal of the ochre.

The electrolysis reactions have an effect on the composition of the filtrate and the efficient use of the current in the system. The species which result from the anodic reactions and their possible complexes (e.g. $Cu(OH)_2$ and CuBr) may be insoluble in the liquid phase. The presence of insoluble products from a reaction of the copper ions with hydroxide or bromide ions is examined using estimates of the solubility product. If all of the current available in the process were used in the corrosion of the anode, Faraday's law predicts the rate of corrosion as

$$\frac{W}{t} = \frac{IA}{zF} \quad (16)$$

where W is the weight in grams of material corroded, t is the time of current application, I is the current, z is the valency, F is Faraday's constant, and A is the atomic weight of the metal. Solubility product calculations for the maximum and minimum values of current indicate that at the pH of the filtrate, the solubility product is exceeded for the complexes of copper. However, these calculations assume that the species in the solubility product are the only species in solution.

Industrial systems containing complex mixtures of anions and cations result in complex electrode reactions. Lockhart [20] reported a variation in the effect of added electrolyte on the electro-osmotic dewatering of sodium kaolinite for washed and unwashed samples. In our research all electro-

TABLE 3

Concentration range of colored filtrate production during electro-osmotic dewatering

NaOH conc. (M)	CTAB conc. (M)				
	0.0	$5.0 \cdot 10^{-4}$	$9.0 \cdot 10^{-4}$	$2.5 \cdot 10^{-3}$	$5.0 \cdot 10^{-3}$
$9.0 \cdot 10^{-4}$	CLEAR FILTRATE				
$2.5 \cdot 10^{-3}$					
$5.0 \cdot 10^{-3}$					
$7.0 \cdot 10^{-3}$	BROWN FILTRATE				
$9.0 \cdot 10^{-3}$					

osmotic dewatering experiments were conducted on unwashed ochre slurries from the mining facility. Hence, although electrolysis may generate different species during electro-osmotic dewatering, the system used in this work may have contained a variety of ions from the hydraulic mining operation.

A number of researchers have reported the chemical reactions that may occur in an iron oxide system. Early work by Smith and Kidd evaluated the stability of iron oxide in the form of goethite (α-FeO·OH) in neutral and alkaline solutions under pressure [21]. Smith and Kidd also discovered that the decomposition point of iron oxide is difficult to locate near neutrality, the area of operation of this present work, owing to the insolubility of iron oxide in water. Another study by Picard et al. studied the electrochemical reduction of iron oxide suspensions in a mixture of water and sodium hydroxide [22]. However, in results similar to those of Smith and Kidd, Picard found that the transformation of goethite into ferrate(III) and hematite occurs, beginning at temperatures of 90°C and 140°C respectively.

The aforementioned results on the chemical transformation of iron oxides suggest that the presence of a brown filtrate in the current electro-osmotic dewatering experiments is not due to a decomposition reaction. This observation is supported by the information provided by the manufacturer of the ochre which states that the ochre is lightfast, insoluble in water, and resistant to alkali and weak acids. In addition, the estimated amount of water-soluble material in the ochre is 0.5–2.5%. The brown color observed in the filtrate may be partially due to the presence of copper (Cu, red) or cuprous oxide (Cu_2O, red) resulting from electrolysis. However, it is possible that any free iron present reacts to form iron oxide (Fe_2O_3, red) or that Fe_2O_3 reacts to form hydrous iron oxide, $Fe(OH)_3$, which is reddish brown.

Another explanation for the generation of a colored filtrate is a change in the physical properties of the ochre upon addition of a dispersant. It has been determined in this work, by both capillary suction time information and the corresponding decrease in vacuum flow rates, that the addition of sodium hydroxide to the ochre slurry causes the deflocculation or dispersal of the particles. In the event that the suspended brown material was colloidal in nature, it would not settle out under the influence of gravity alone, causing the liquid to maintain its brown color over a long period of time.

Conclusions

Electro-osmotic separation is a process that can be implemented in conjunction with conventional methods of dewatering to enhance the extent and rate of dewatering of ultrafine slurries. Measured zeta potentials for the untreated slurry were zero, confirming the absence of an electro-osmotic driving force. In dewatering tests conducted with CTAB alone on slurries exhibiting hydrophobic behavior, there was a slight increase in the rate and extent of hydraulic dewatering with increasing CTAB concentration.

The adsorption of hydroxide ions increased the negative zeta potential, causing an electrostatic dispersal of the particles and producing a less porous cake which inhibited hydraulic flow rates. In the absence of CTAB the measured zeta potential values increased from zero for the slurry in the absence of chemical additives, to −42.1 mV at a NaOH concentration of $9 \cdot 10^{-3}$ M.

CTAB assisted in the hydraulic dewatering of the base-treated iron oxide slurries by (1) flocculating the dispersion through hydrophobic interactions of the non-polar portion of the CTAB molecule and (2) reducing the surface tension produced by the addition of surfactant with an overall decrease in the capillary pressure drop (lower CST and improved hydraulic dewatering). This was qualitatively measured using the capillary suction time apparatus.

Electrostatic adsorption of excess CTA^+ ions can diminish or eliminate the electro-osmotic effects of the hydroxide ions with an associated

reduction in electro-osmotic dewatering. In addition, subsequent increases in CTAB concentration may result in charge reversal of the particles through the mechanism of multilayer adsorption. The use of both NaOH and CTAB as surface conditioning agents promotes a synergistic reduction (over 40%) in the final cake moisture content during combined hydraulic and electro-osmotic dewatering.

The extension of surfactant-enhanced electro-osmotic dewatering to other uncharged ultrafine dispersions requires an evaluation of the electrical and hydraulic parameters (e.g. zeta potential and specific resistance) of the particular system. The presence of foreign chemical species in ultrafine particle dispersions may invalidate the predicted electrokinetic behavior by altering the surface conductivity and the zeta potential. Furthermore, the chemical additive should (1) be surface active, (2) not react chemically with other chemical species in the system, and (3) avoid the significant dispersion of particles if hydraulic separation techniques are being utilized.

Acknowledgments

The authors wish to acknowledge support of this project by the Bureau of Mines, U.S. Department of the Interior, Allotment Grant no. G1194113. The contents do not necessarily reflect the views and policies of the U.S. Bureau of Mines. Mention of commercially produced instruments and products does not constitute endorsement or recommendation for use by the U.S. Bureau of Mines.

References

1 J.G. Sunderland, J. Appl. Electrochem., 17 (1987) 889.
2 N.C. Lockhart, Int. J. Miner. Process., 10 (1983) 131.
3 D.J. Kelsh and R.H. Sprute, Drying Technol., 1 (1984) 57.
4 R.H. Sprute and D.J. Kelsh, U.S. Bur. Mines, Rep. Invest. 8666, 1982.
5 J. Greyson, Yale Sci. Mag., XLIV (1970) 6.
6 H. Yukawa, H. Yoshida, K. Kobayashi and M. Hakoda, J. Chem. Eng. Jpn., 11 (1978) 475.
7 D. Ellis and J.G. Sunderland, NTIS Report no. PB-276 412, 1977, 24 pp.
8 D.J. Shaw, Electrophoresis, Academic Press, London, 1969.
9 R.J. Hunter, Zeta Potential in Colloid Science: Principles and Applications, Academic Press, London, 1981.
10 R.C. Baskerville and R.S. Gale, Water Pollut. Control, 67 (1968) 233.
11 P.A. Vesilind, J. Water Pollut. Control Fed., 60 (1988) 215.
12 I. Iwasaki, S.R.B. Cooke and H.S. Choi, Am. Inst. Min. Met. Pet. Eng. Trans., 217 (1960) 237.
13 C.S. Grant and E.J. Clayfield, Surfactant-enhanced electro-osmotic dewatering in mineral processing, in Y.A. Attia, B.M. Moudgil and S. Chander (Eds), Interfacial Phenomena in Biotechnology and Materials Processing Proceedings, Boston, MA, August 3–7, 1987, Elsevier, Amsterdam, 1988.
14 C.S. Grant, Surfactant-enhanced electro-osmotic dewatering of mineral ultrafines, Ph.D. Thesis, Georgia Institute of Technology, Atlanta, GA, 1989.
15 P.G. Johansen and A.S. Buchanan, Aust. J. Chem., 10 (1957) 392.
16 J.T. Davies and E.K. Rideal, Interfacial Phenomena, Academic Press, New York, 1963.
17 E.C. Potter, Electrochemistry—Principles and Applications, Cleaver-Hume, London, 1956.
18 N.C. Lockhart, Electro-dewatering of fine suspensions, in H.S. Muralidhara (Ed.), Advances in Solid–Liquid Separation, Battelle, Columbus, OH, 1986.
19 N.C. Lockhart, Colloids Surfaces, 6 (1983) 229.
20 N.C. Lockhart, Colloids Surfaces, 6 (1983) 239.
21 F.G. Smith and D.J. Kidd, Am. Mineral., 34 (1949) 403.
22 G. Picard, D. Oster and B. Tremillon, J. Chem. Res., (1980) 250.